



e-ISSN: 2319-8753 | p-ISSN: 2347-6710

# IJRSET

International Journal of Innovative Research in  
**SCIENCE | ENGINEERING | TECHNOLOGY**



# INTERNATIONAL JOURNAL OF INNOVATIVE RESEARCH

IN SCIENCE | ENGINEERING | TECHNOLOGY

Volume 13, Issue 5, May 2024

**ISSN** INTERNATIONAL  
STANDARD  
SERIAL  
NUMBER  
INDIA

Impact Factor: 8.423

 9940 572 462

 6381 907 438

 [ijirset@gmail.com](mailto:ijirset@gmail.com)

 [www.ijirset.com](http://www.ijirset.com)

# The Design and Construction of a Wind Turbine with Vertical Axis

Himanshu Khandelwal<sup>1</sup>, Neelabh Gupta<sup>2</sup>, Dr. Barkha Gupta<sup>3</sup>

Assistant Professor, Department of Mechanical Engineering, Modi Institute of Technology, Kota, Rajasthan, India<sup>1</sup>

Assistant Professor, Department of Mechanical Engineering, Modi Institute of Technology, Kota, Rajasthan, India<sup>2</sup>

Associate Professor, Department of Mechanical Engineering, Modi Institute of Technology, Kota, Rajasthan, India<sup>3</sup>

**ABSTRACT:** Vertical axis wind turbines (VAWT) are sought after because the average wind velocity in urban areas is insufficient to operate horizontal axis wind turbines (HAWT). The two types of vertical axis wind turbines are Darrieus (lift) and Savonius (drag). The comparison of the Savonius and Darrieus types of vertical axis wind turbines' coefficient of performance (COP) is the main objective of the current investigation. ANSYS Fluent—Computational Fluid Dynamics (CFD) software—is used to numerically analyze the aforementioned VAWTs. Both turbines have blade designs that are optimized to produce the highest output given the available input. The wind turbines' output parameters are obtained individually and compared for the same input parameters. This comparison offers a foundation for selecting the appropriate VAWT type based on the function.

Keywords: - Vertical Axis Wind Turbine, Ansys Fluent, CFD

## I. INTRODUCTION

The use of various energy sources to generate electricity has resulted in a slew of environmental issues. Renewable energy is gaining a lot of attention as an alternate answer. Wind energy distinguishes out among these renewable resources as being abundant, clean, inexhaustible, and environmentally beneficial.

Windmills were also used to harness renewable power in farming for irrigation and grain milling for ages. Wind energy can be captured from all directions with the axis of rotation directed vertically in Vertical Axis Wind Turbines (VAWT), but are an older wind turbine type. In general, VAWTs are divided into two types: drag-type and raise-type. A Savonius rotor with concave or concave-shaped blades could be a popular drag type VAWT. To induce the move motion, it uses the mechanics forces to go on the advancing blade. The rotors are driven by the lift component generated by the pressure difference on each side of the Darrieus rotor and H-rotor with surface-shaped blades in lift-type VAWTs like the Darrieus rotor and H-rotor with surface-shaped blades.

## II. DESIGN OF BLADES

### 2.1 Darrieus Rotor

A vertical rotating shaft holds several curved aero foil blades that make up the Darrieus wind turbine. Only at high rotation speeds can a blade be stressed in tension due to its curvature. The aero foils move in a circular motion through the air as the Darrieus rotor spins. A part of the lift force rotating in the direction of the wind extracts the energy from it. Utilizing software tools, aerodynamic modeling is created with the NACA0021 aero foil. Figure 1

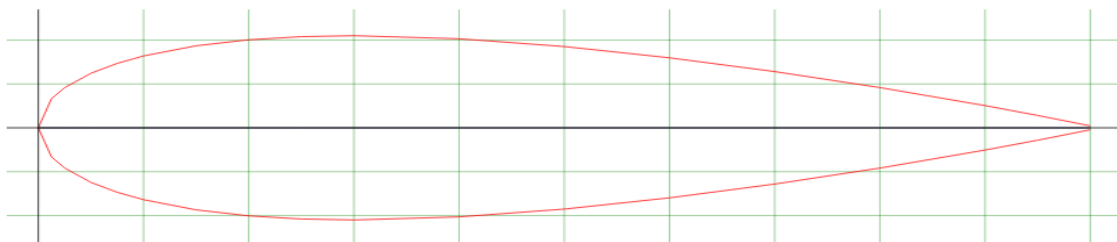


Figure 1 NACA0021

## 2.2 Savonius Rotor

Among the simplest turbines is the Savonius turbine. It is a drag-type device with two or three blades in terms of aerodynamics. The curvature reduces drag on the blades when they move against the wind as opposed to when they move with it. The Savonius turbine rotates due to differential drag. The wind turbine models' rotor rotation is affected by several blades. Compared to wind turbines with two or four blades, the one with three blades generates a higher rotational speed and tip speed ratio.

## III. MEHTODS

### 3.1 CONFIGURATION AND NUMERAL MODEL

A two-bladed H-rotor VAWT with a NACA 0021 airfoil was used in the experiment. The VAWT's height ( $H$ ) and diameter ( $D$ ) were 1200 mm and 2000 mm, respectively, while the blade's chord length ( $c$ ) was 265 mm with a pitch angle ( $\beta$ ) of  $6^\circ$ . The pitch angle is the angle formed by the chord line and the tangential line, as shown in Fig. 1(a). The turbulence intensity of the wind tunnel during the test was 0.5 percent. The torque and aerodynamic performance were evaluated using a torque meter and Laser Doppler Velocimeter (LDV), while the pressure distribution was monitored using 32 wireless pressure taps attached to one of the rotors blades, according to Li et al.

### 3.2 CFD Spatial Realm Discretization & Extremities condition:

For the simulation, sub-domain names have been modeled: a cuboid for the tunnel stator and a cylinder for the VAWT rotor. Shown in Fig. 2 are the pinnacle view and the facet view of the area with the boundary situation applied. The tunnel stator area became modeled with inside the size of  $10D$  (width)  $\times$   $10D$  (height)  $\times$   $25D$  (length) while the VAWT rotor domain was characterized by a rotational diameter  $1.5D$  and  $0.2$  m gaps for the top and bottom VAWT rotor domain was located at  $10D$  from the inlet and  $15D$  from the outlet to allow full development of wakes. A VAWT with a smaller domain size of  $10D$  (width)  $\times$   $8D$  (height)  $\times$   $16D$  (length) with the rotor domain  $5D$  from the inlet.

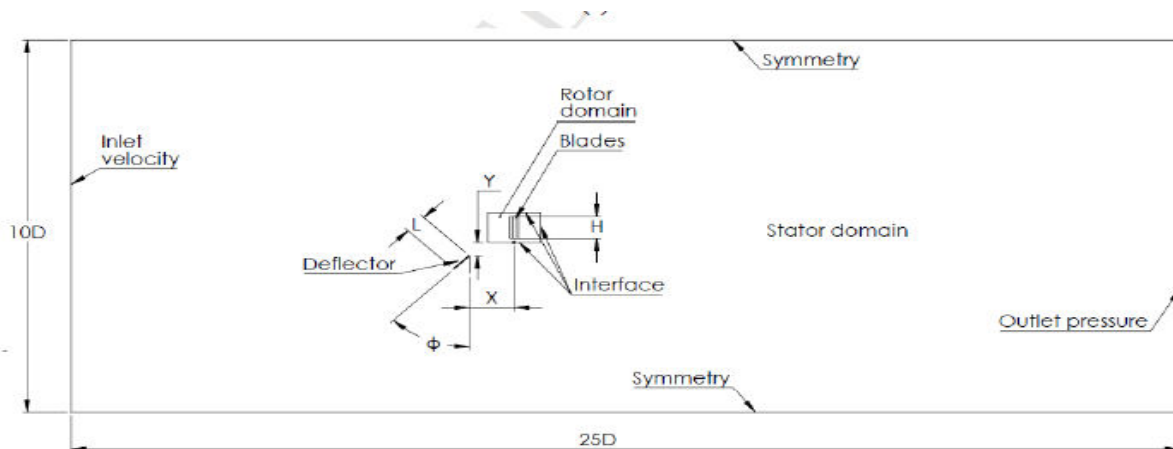


Fig. 2 Geometry of Model

The 2 bladed H-rotor VAWT turned into modeled with inside the rotor domain. at the same time as the flat plate deflector turned into placed on the stator tunnel domain. The flat plate deflector turned into positioned at a horizontal distance,  $X$  from the rotational axis and a vertical distance,  $Y$  from the lowest fringe of the VAWT. The duration of the flat plate deflector turned into denoted with the aid of using  $L$  and the inclination attitude of the flat plate deflector from the vertical aircraft turned into denoted with the aid of using  $\phi$ . This value is suggested to be less than 6%-7.5% for numerical simulation and 10 % for experiment. In this simulation, the blockage issue for the VAWT was solely 0.6% and 4.2% for the case with the most important size of the device system; each fell at intervals the appropriate vary. Since the simulation aimed to reproduce the results of the wind tunnel test, a uniform wind inlet velocity of 8 m/s, turbulence intensity of 0.5%, length scale of 18.55 mm The TSR of the benchmark experiment is 2.58,  $Re = 3.27 \times 10^5$ . The straight-bladed VAWT with inside the rotor area rotates clockwise with  $\omega = 20.64$  rad/s.

#### IV. SOLVER SETTINGS

The 3D simulation for solving the time-dependent Unsteady Reynolds Averaged Navier Stokes (URANS) problem using the pressure based formulation was performed using the commercial programme ANSYS Fluent, which is based on the finite volume method. The Navier-Stokes equation is solved using this approach. The fluid in the simulation was air, with the default parameters of density of 1.225 (kg/m<sup>3</sup>) and viscosity of 1.789410-5 (kg/msec). ANSYS Fluent was used to simulate and observe torque coefficients on a single blade of the VAWT in all scenarios. The force coefficients were calculated repeatedly until convergent values were obtained for two consecutive revolutions with disagreement percentages of less than 1%, as follows:

##### 1. Mesh independency test:

The mesh files for the simulations were generated using the CFD programme included with ANSYS Fluent. To make meshing easier, two mesh domain files (VAWT rotor and tunnel stator) were created separately. Meshes were re-attached in the solver stage using the appended function in the programme, and the VAWT rotor domain was incorporated within the tunnel stator domain.

##### 2. Deflector system & parameters:

A few flat plate deflector settings were investigated for the study of flow characteristics and the effect of the flat plate deflector on the VAWT, including

1. The X-distance (horizontal distance from the rotational axis)
2. The Y-distance (vertical distance between the lower edge of VAWT and the top edge of the flat plate deflector)
3. Angle of inclination,  $\phi$
4. The flat plate deflector's Length L

The flat plate deflector was installed upwind of the VAWT, as shown in Figure. To investigate the impacts of the flat plate deflector's position, four X distances were simulated:  $X = 0$  (at the rotor axis),  $R$ ,  $2R$ , and  $3R$ . Other parameters were set at  $Y = 1/3H$ ,  $\phi = 0^\circ$ , and  $L = H$  at the same time. The effect of the vertical Y distance, which varied from  $Y = 0$ ,  $1/3H$ ,  $2/3H$ , and  $H$ , as shown in Fig., was tested using the X distance that showed the highest CT, average. Angles of  $0^\circ$ ,  $30^\circ$ ,  $45^\circ$ , and  $60^\circ$  were also examined to determine the optimal position of the. Finally, there is the simulation. The effects of the flat plate deflector length as a factor, which was varied from  $L = 0.5H$ ,  $1H$ ,  $1.5H$ , and  $2H$ , followed by the effects of the flat plate deflector length as a factor, which was varied from  $L = 0.5H$ ,  $1H$ ,  $1.5H$ , and  $2H$ . In all situations, the flat plate deflector plate's width and thickness were set to  $3D$  and  $10$  mm, respectively, to cover the VAWT's diameter.

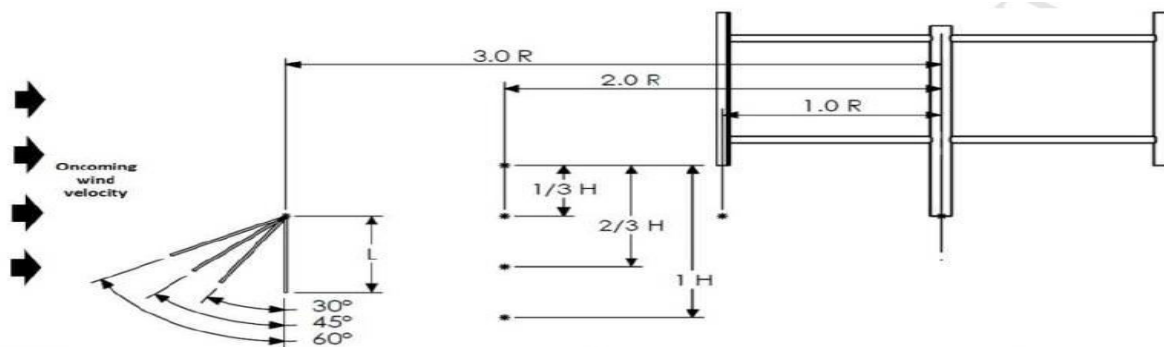


Fig.3 Various parameters of the flat plate deflector

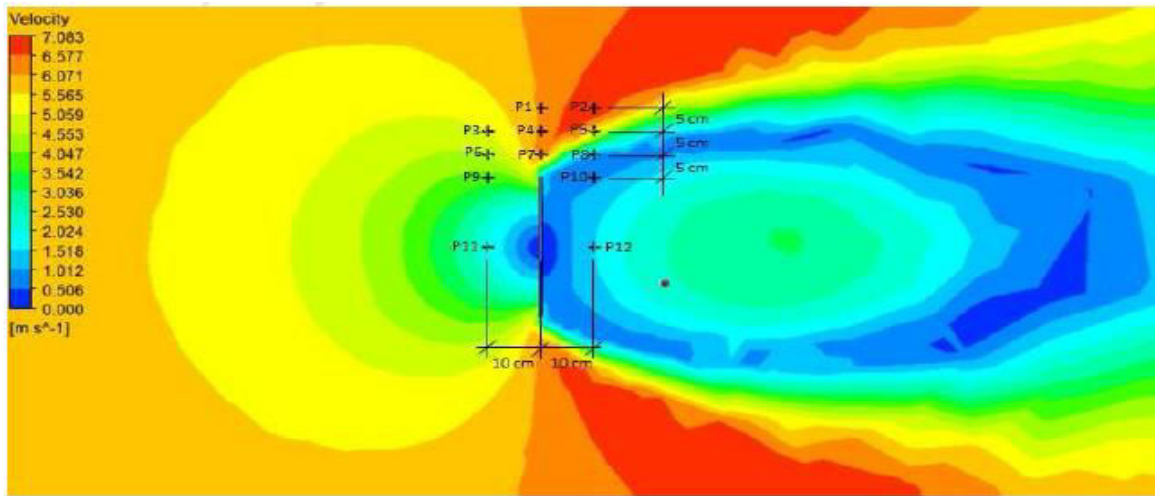


Fig 4 Velocity measurement points around the flat plate deflector

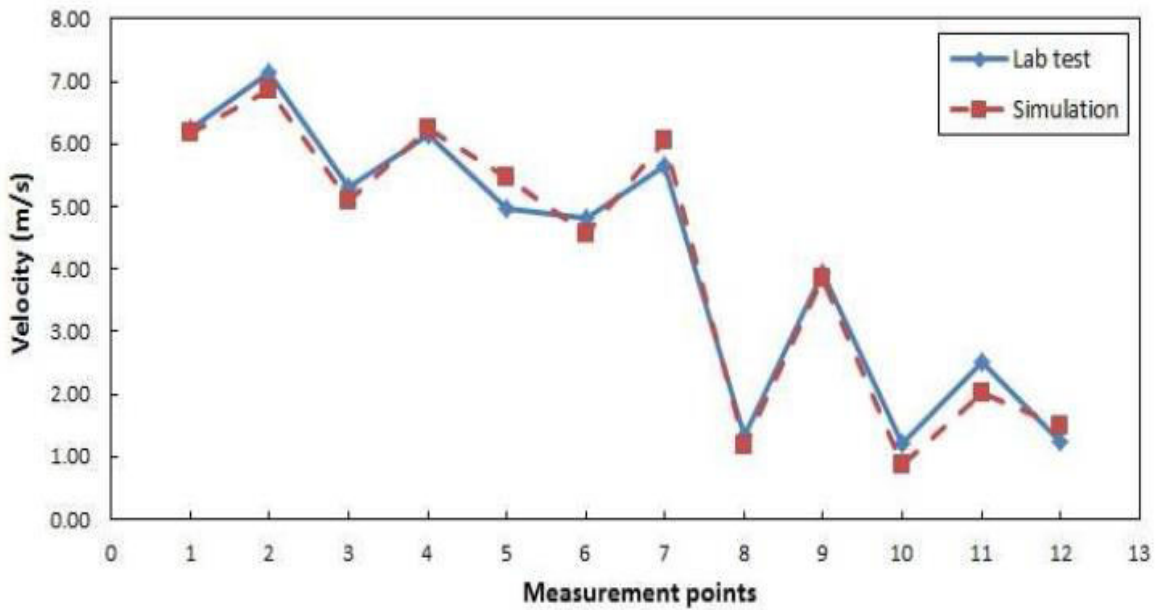


Fig.5 Experiment and simulation results for the velocity 409 measurement

### V. RESULTS AND DISCUSSION

The process involves in chapter makes the analysis and finds result. During this chapter we'll discuss the results output of the various stages involve in the analysis.

#### 5.1 Simulation:

The CFD simulation was validated by the wind tunnel test data. The COP ( $C_p$ ) ata from the test was obtained at each 5° azimuth angle, thus a total of 72 data to show the curve for a full revolution of the VAWT at TSR 2.58.

The simulation result observed that for a complete revolution there are two peaks in  $\theta$ , approximately equal to 90° and 225°, and two valleys at approximately 0° and 180°. In pattern, the bend is affected by the shifting approach and the resultant breeze stream. The primary sharp peak accomplishes a high greatness of  $C_p$  when the edge goes at the direction of air where the approach is ideal. The another peak at  $\theta = 225^\circ$  which has more extensive and much lesser

than the first, emerges from the sharp edge cooperating with the wake created by the cutting edge itself at the direction of air moving to the downwind. Thus, the force made at the upwind ends up being a lot more noteworthy than the downwind. The box of the bend seem when the rotor edge is corresponding to the free stream and the approach is zero.

It's additionally seen that there are a few inconsistencies particularly at  $\theta$  between  $220^\circ - 35^\circ$ . As per the recreation performed by Li. et al., similar errors happened. This was because of the impact of the prompted speed which was produced from the tip vortex. The lower and negative worth got from the reenactment was because of the overall approach is lower than the slow down point in light of the impact of the edge tip 431 vortex in the air stream explore. The stream at the downwind district was extremely perplexing from the impact of the sharp edge going through the upwind area. Moreover, the rearrangements of the math in the demonstrating additionally added to the disparities As detailed in the writings which led reenactment on NACA series of airfoil, comparable patterns were gotten at  $\theta$  between  $230^\circ - 45^\circ$ .

In the addition to the power coefficient validation, the pressure distribution on the blade surface was examined by comparing the pressure coefficients,  $C_{Pressure}$  Fig. 6 and Fig. 7 illustrate the pressure distribution at azimuthal angle of  $445^\circ 0^\circ, 90^\circ, 180^\circ$  and  $270^\circ$ . It can be observed that the distribution of pressure of the rotor blade 446 from the simulation follows the trend from the experiment well.

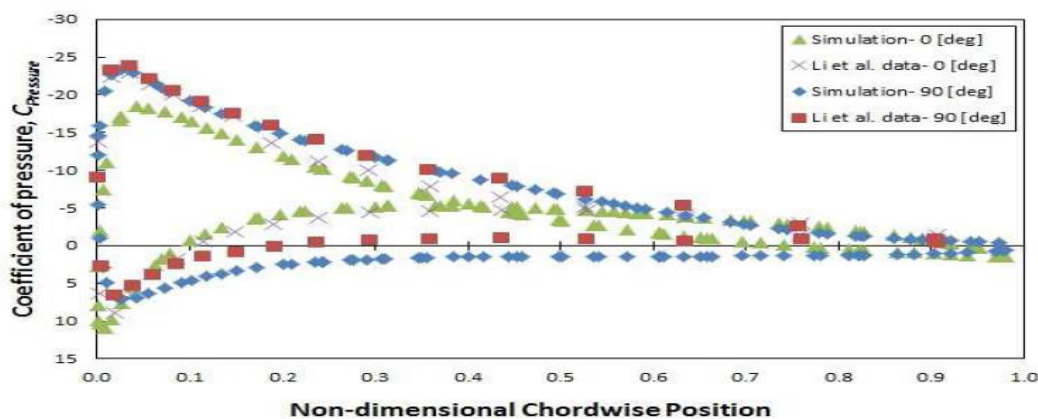


Fig. 6 Pressure coefficient on the blade surface at  $\theta = 0^\circ$  and  $90^\circ$  at TSR= 2.58.

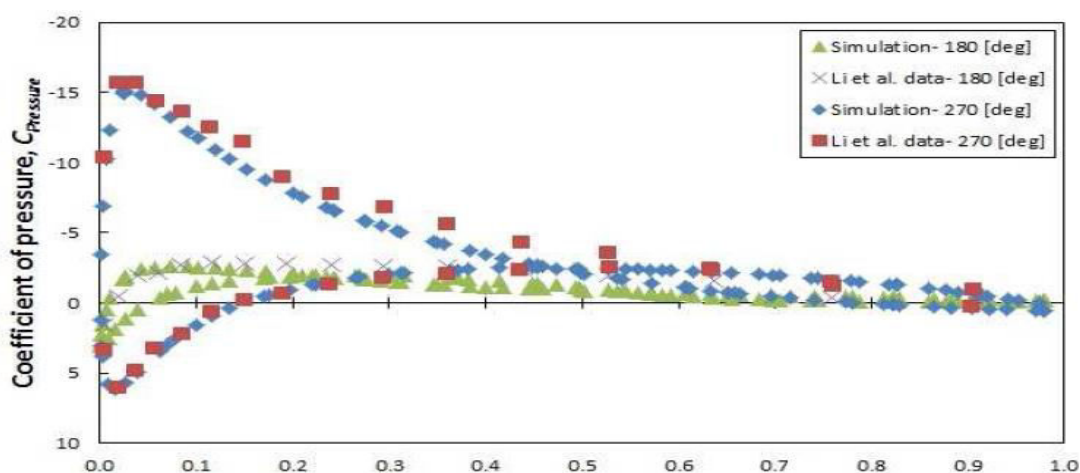


Fig.7 Pressure coefficient on the blade surface at  $\theta = 180^\circ$  and  $270^\circ$  at TSR= 2.58.

**5.2 Deflector System Effects:**

**5.2.1 X distance Effects:**

With the check of the reproduction arrangement, the impact of a level plate deflector was researched. From the reproduction results, it showed that the presence of the level plate redirector had the option to work on the exhibition of the VAWT essentially; in any case, it was exceptionally reliant upon the place of the deflector.

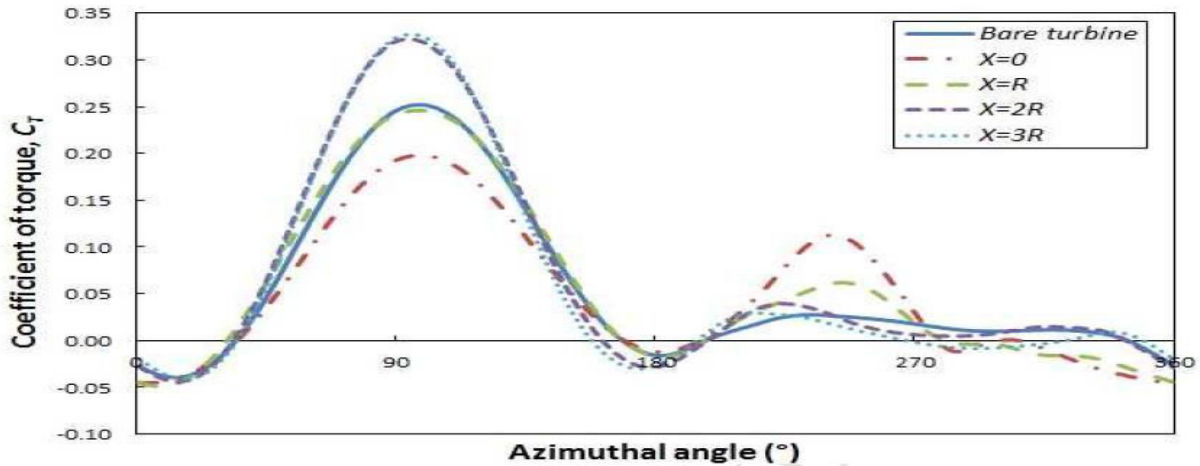


Fig. 8 Torque Coefficient for various X distances with  $Y = 1/3 H$ ,  $\phi = 469 0^\circ$  and  $L = 1.0 H$

**5.2.2 Y distance Effects:**

Since when  $X = 2R$  appeared the most excellent comes about, in this manner it was settled to examine the Y separate impacts. The Y separate is the separate between the lower edge of the VAWT and the upper edge of the level plate redirector and it was shifted from  $Y = 0, 1/3H, 2/3H$  and  $H$ . As appeared in Fig. 16, a comparable slant with the X remove was watched where the deflector opened up the wind stream speed coming to the VAWT altogether. Too, when the redirector was set as well close to the VAWT, a subpar execution was gotten. For the case  $Y = 0$ , the CT, ave esteem for all  $\theta$  diminished definitely.

As the diverter was set advance from the VAWT, at  $Y = 1/3H, 2/3H$  and  $H$ , good enlargement impacts were watched. At  $\theta = 90^\circ$  and  $200^\circ$ , an moved forward CT was obtained compared to the uncovered turbine as appeared in Fig.9. This was basically due to the tall velocity wind which was avoided towards the VAWT particularly at the upwind locale. In addition, the wake impacts were moved down and absent from the VAWT when the Y remove expanded.

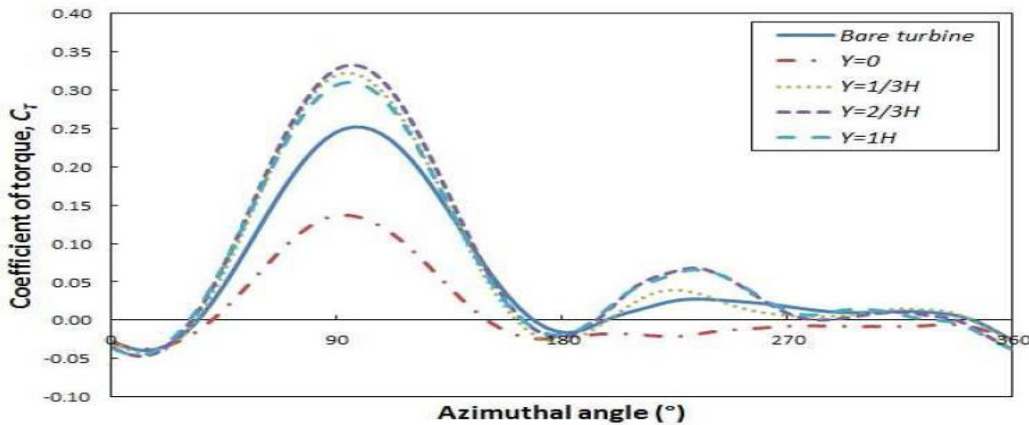


Fig. 9 Torque Coefficient for various Y distances with  $X = 2 R$ ,  $\phi = 543 0^\circ$  and  $L = 1.0 H$

**5.2.3 Flat Plate Deflector Effects inclination angle,  $\phi$ :**

In the recreation was proceeded in arrange to think about the impacts of the slant point,  $\phi$  with the position  $X = 2R$  and  $Y = 2/3H$ . From Fig. 18, as the slant point increments, the expansion impacts ended up less noteworthy, particularly at the upwind locale. The  $C_T$ , average values for diverse slant points of the redirector are organized in Table 4, showing that the most extreme  $C_T$ , average was gotten when the diverter has no slant ( $\phi = 0^\circ$ ) which was 32.61% higher than the bare turbine.

**5.2.4 Flat Plate Deflector Effects length, L:**

For the last boundary of the recreation, the length of the redirector plate was changed from  $L = 0.5H, 1.0H, 1.5H, 2.0H$  with different boundaries fixed as  $X = 2R, Y = 2/3H$  and  $\phi = 0^\circ$ . All cases gave an improved outcome contrasted with the uncovered turbine. As the length  $L$  builds, the  $C_T$ , are increments until the ideal length where  $L = 1.5H$ . The  $C_T$ , average accomplished was 0.0820 contrasted with the uncovered turbine, 0.0588; it was around 47.10% addition. Further expanding the length to  $L = 2.0H$ , the  $C_T$ , average marginally decreased to 0.0800, yet still around 43.40% higher than the exposed turbine.

From the recreation results, the boundaries which yield the best outcomes happened when  $X = 2R, Y = 2/3H, \phi = 0^\circ$  and  $L = 1.5H$ . Nonetheless, these boundaries were restricted for a particular kind of wind turbine. Different variables including the robustness and the angle proportion are great to consider later on study. As previously mentioned, the  $C_T$  values acquired from the reproductions are just for the single rotor sharp edge. To compute the general exhibition of the 2-straight bladed VAWT, the  $C_T$  diagram is counterbalanced by an azimuth point of  $180^\circ$  for the second sharp edge blade. The simulated  $C_T$  values for blade 1, blade 2, and the total 630 sum of the  $C_T$  values at each azimuth angle for the best case. Under this condition, the total 631  $C_T$ , ave value was 0.1640, corresponding to the  $CP$ , ave of 0.4231.

**5.3 Designed 3D of VAWT:**

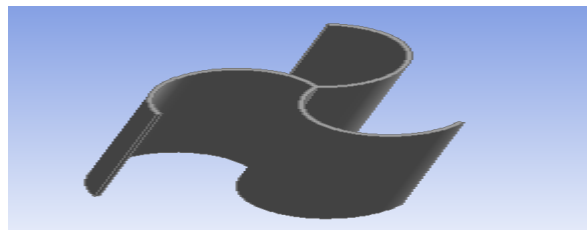


Figure 10 depicts the 3D design of VAWT, which was created using the ANSYS Design Modeller. To determine turbine pressure, this design will also be simulated using ANSYS. Fluid Flow (Fluent) from ANSYS is used to perform CFD analysis. Import Geometry from programme like Solid Works or AutoCAD as the initial step. We can design it using the Designer Design supplied by ANSYS in addition to importing it from design programme.

**5.4 Designer 2D Top View VAWT Using Design Modeler**

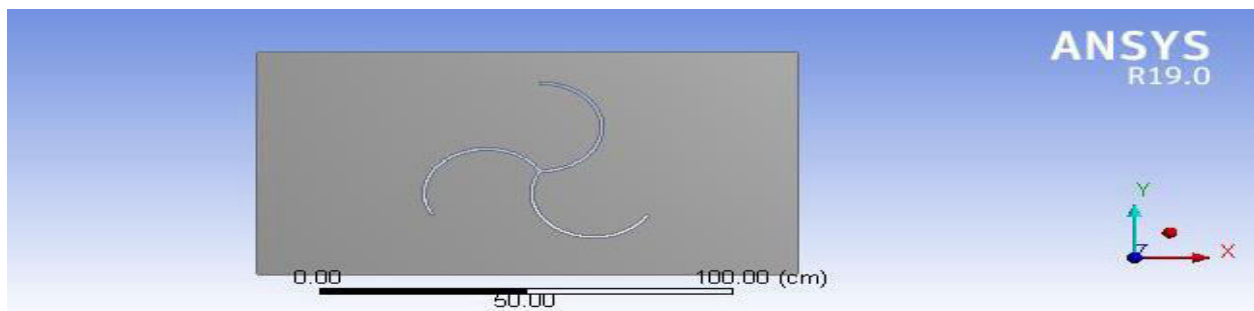
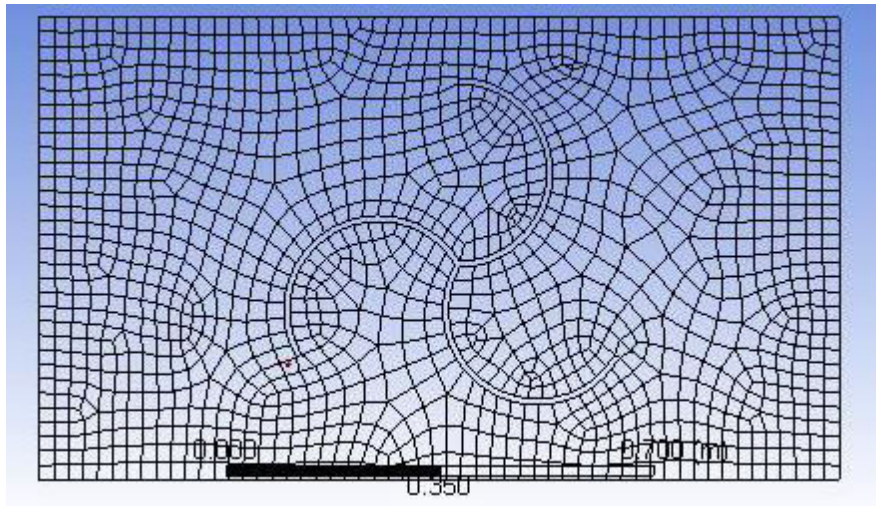


Figure 11 is a 2D top view of a VAWT design created with Design Modeler. To analyze fluently, we must execute the Meshing procedure after creating or importing geometry. We can choose Mesh on the fluid flow to start the meshing process right now. The meshing procedure will then proceed in accordance with the existing geometry.

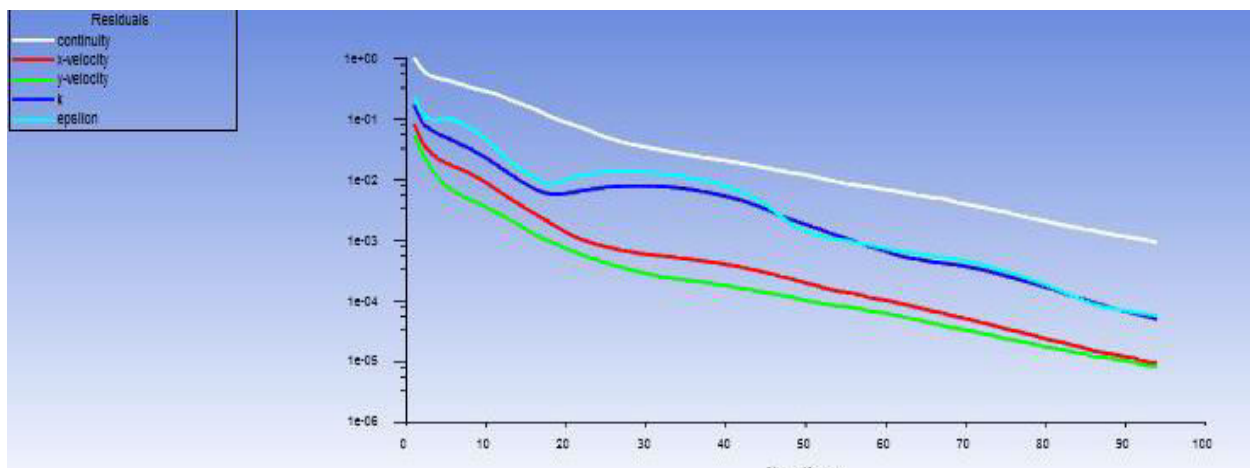
### 5.5 Meshing Geometry on ANSYS

On ANSYS Fluent, Meshing Geometry is shown in Figure 12 after you've completed all of the stages, you can set up to receive the solution you want. Figure 1 depicts the findings in this paper.



### 5.6 Iterations

The number of iterations conducted by the solvent is shown in Figure 13. The solvent specifies 200 iterations for convergence, but the solution actually converged at 95 iterations. We can see Velocity & Pressure Contours after they have converged.



## VI. CONCLUSIONS

The streamlined exhibition of a NACA0021 straight-bladed vertical hub wind turbine with a level plate diverter was examined utilizing CFD reproductions. The CFD reenactment was first approved by the air stream testing information from the writing. Subtleties of the reenactment arrangement, fitting philosophy, and time step choice are depicted. The reproduction results showed a decent concurrence with the air stream try. Additionally, the impacts of a level plate redirector put at the upwind of the VAWT were researched. From the review, the level plate redirector fills in as a power increase element to work on the presentation of the VAWT by diverting and speeding up the breeze stream towards the VAWT. The breeze at the close to wake district was around 20% higher than the approaching breeze stream. Be that as it may, it was exceptionally subject to the position. A couple of boundaries of the level plate redirector were explored for their impacts on the general execution of the VAWT including the X and Y position at upwind, the tendency point and the length of the diverter. From the reenactments, it tends to be presumed that the best cycle-arrived at the midpoint of CT with a acquire of around 47.10% happens when the redirector was put at an upwind distance 2R from the rotor shaft, 2/3H from the base edge of the rotor edges, no tendency point and with a redirector length of 1.5H. This level plate redirector is appropriate and simple to be retrofitted on the existing VAWT

framework to additional increment the power yield. This study was completed under the condition where the redirector worked in a solitary breeze stream heading.

## VII. FUTURE SCOPE

For future review, An Omni-heading element can be brilliantly planned and examined to support the ability of a VAWT in catching additional breeze energy from various headings. Additionally, the current examination was done on a particular kind of VAWT which viewpoint proportion around 1. It is important to concentrate on the impacts of the perspective proportion for the redirector and the VAWT in future.

## REFERENCES

- [1] Kok Hoe Wong, Wen Tong Chong,\*, Sin Chew Poh, Yui-Chuin Shiah, Nazatul Liana Sukimana, Chin-Tsan Wangc “3D CFD Simulation and Parametric Study of a Flat Plate Deflector for Vertical Axis Wind Turbine” *Renewable Energy* (2018), doi: 10.1016/j.renene.2018.05.085.
- [2] X. Jin, G. Zhao, K. Gao, W. Ju, Darrieus vertical axis wind turbine: Basic research 715 methods, *Renewable and Sustainable Energy Reviews* 42 (2015) 212-225.
- [3] Jin X, Zhao G, Gao K, Ju W. Darrieus vertical axis wind turbine: Basic research methods. *Renewable and Sustainable Energy Reviews*, 2015; 42(1):212-225.
- [4] T. Ackermann, L. Söder, An overview of wind energy-status 2002, *Renewable and sustainable energy reviews* 6 (1-2) (2002) 67–127.
- [5] R. Gasch, J. Twele, *Wind power plants: fundamentals, design, construction and operation*, Springer Science & Business Media, 2011.
- [6] E. W. Golding, R. Harris, *The generation of electricity by wind power*, E. & FN Spon London, 1976.
- [7] J. F. Manwell, J. G. McGowan, A. L. Rogers, *Wind energy explained: theory, design and application*, John Wiley & Sons, 2010.
- [8] S. S. Johannes, Rotor adapted to be driven by wind or flowing water, uS Patent 1,697,574 (Jan. 1 1929).
- [9] S. J. Savonius, Wind rotor, uS Patent 1,766,765 (Jun. 24 1930).
- [10] D. G. J. Marie, Turbine having its rotating shaft transverse to the flow of the current, uS Patent 1,835,018 (Dec. 8 1931).
- [11] J. N. Sorensen, W. Z. Shen, Computation of wind turbine wakes using combined navier- stokes/actuator-line methodology, in: 1999 European Wind Energy Conference and Exhibition, 1999, pp. 156–159
- [12] R. Howell, N. Qin, J. Edwards, N. Durrani, Wind tunnel and numerical study of a small vertical axis wind turbine, *Renewable Energy* 35(2) (2010) 412-422.
- [13] M.S. Siddiqui, N. Durrani, I. Akhtar, Quantification of the effects of geometric approximations on the performance of a vertical axis wind turbine, *Renewable Energy* 74 (2015) 661-670.
- [14] H.F. Lam, H.Y. Peng, Study of wake characteristics of a vertical axis wind turbine by two- and three-dimensional computational fluid dynamics simulations, *Renewable Energy* 90 (2016) 386-398.
- [15] G. Bedon, S. De Betta, E. Benini, A computational assessment of the aerodynamic performance of a tilted Darrieus wind turbine, *Journal of Wind Engineering and Industrial Aerodynamics* 145(Supplement C) (2015) 263-269
- [16] A.M. Chowdhury, H. Akimoto, Y. Hara, Comparative CFD analysis of Vertical Axis Wind Turbine in upright and tilted configuration, *Renewable Energy* 85 (2016) 327-337.
- [17] M.H. Mohamed, G. Janiga, E. Pap, D. Thévenin, Optimal blade shape of a modified Savonius turbine using an obstacle shielding the returning blade, *Energy Conversion and Management* 52(1) (2011) 236-242.
- [18] K. Golecha, T.I. Eldho, S.V. Prabhu, Influence of the deflector plate on the performance of modified Savonius water turbine, *Applied Energy* 88(9) (2011) 3207-3217.
- [19] B.D. Altan, M. Atilgan, The use of a curtain design to increase the performance level of a Savonius wind rotors, *Renewable Energy* 35(4) (2010) 821-829.
- [20] D. Kim, M. Gharib, Efficiency improvement of straight-bladed vertical-axis wind turbines with an upstream deflector, *Journal of Wind Engineering and Industrial Aerodynamics* 115 (2013) 48-52.
- [21] X. Jin, Y. Wang, W. Ju, J. He, S. Xie, Investigation into parameter influence of upstream deflector on vertical axis wind turbines output power via three-dimensional CFD simulation, *Renewable Energy* 115 (2018) 41-53.
- [22] Q.a. Li, T. Maeda, Y. Kamada, J. Murata, K. Furukawa, M. Yamamoto, The influence of flow field and aerodynamic forces on a straight-bladed vertical axis wind turbine, *Energy* 111 (2016) 260-271.
- [23] P. Marsh, D. Ranmuthugala, I. Penesis, G. Thomas, The influence of turbulence model and two and three-dimensional domain selection on the simulated performance characteristics of vertical axis tidal turbines, *Ren*



INTERNATIONAL  
STANDARD  
SERIAL  
NUMBER  
INDIA



# INTERNATIONAL JOURNAL OF INNOVATIVE RESEARCH

IN SCIENCE | ENGINEERING | TECHNOLOGY

 9940 572 462  6381 907 438  [ijirset@gmail.com](mailto:ijirset@gmail.com)



[www.ijirset.com](http://www.ijirset.com)

Scan to save the contact details